Cortical Membrane Potential Signature of Optimal States for Sensory Signal Detection

Highlights

- Optimal performance of mice on an auditory detection task occurs at moderate arousal

- Large, reliable sub- and supra-threshold sensory responses occur at moderate arousal

- Hyperpolarized, quiescent membrane potentials precede correct detection events

- Pupil diameter predicts cortical dynamic states governing detection task performance

Authors

Matthew J. McGinley, Stephen V. David, David A. McCormick

Correspondence

matthew.mcginley@yale.edu (M.J.M.), david.mccormick@yale.edu (D.A.M.)

In Brief

McGinley et al. reveal the cortical membrane potential dynamics underlying the classically-observed inverted-U dependence of detection task performance on arousal (measured using pupillometry). Optimal arousal exhibits large, reliable sensory-evoked spiking and postsynaptic potentials responses and hyperpolarized, quiescent background membrane potentials.

CrossMark

CellPress

Article

Cortical Membrane Potential Signature of Optimal States for Sensory Signal Detection

Matthew J. McGinley,[1,*] Stephen V. David,[2] and David A. McCormick[1,*]
[1]Department of Neurobiology, Kavli Institute for Neuroscience, Yale University School of Medicine, 333 Cedar Street, New Haven, CT 06510, USA
[2]Oregon Health & Science University, MS: L335A, 3181 SW Sam Jackson Park Rd, OHRC, Portland, OR 97239, USA
*Correspondence: matthew.mcginley@yale.edu (M.J.M.), david.mccormick@yale.edu (D.A.M.)
http://dx.doi.org/10.1016/j.neuron.2015.05.038

SUMMARY

The neural correlates of optimal states for signal detection task performance are largely unknown. One hypothesis holds that optimal states exhibit tonically depolarized cortical neurons with enhanced spiking activity, such as occur during movement. We recorded membrane potentials of auditory cortical neurons in mice trained on a challenging tone-in-noise detection task while assessing arousal with simultaneous pupillometry and hippocampal recordings. Arousal measures accurately predicted multiple modes of membrane potential activity, including rhythmic slow oscillations at low arousal, stable hyperpolarization at intermediate arousal, and depolarization during phasic or tonic periods of hyper-arousal. Walking always occurred during hyper-arousal. Optimal signal detection behavior and sound-evoked responses, at both sub-threshold and spiking levels, occurred at intermediate arousal when pre-decision membrane potentials were stably hyperpolarized. These results reveal a cortical physiological signature of the classically observed inverted-U relationship between task performance and arousal and that optimal detection exhibits enhanced sensory-evoked responses and reduced background synaptic activity.

INTRODUCTION

The cortical subthreshold membrane potential and synaptic dynamics underlying optimal sensory signal detection are not well known. Human and animal studies have reported that performance on signal detection tasks is highly state-dependent, exhibiting an inverted-U dependence on arousal and the activity of neuromodulatory pathways. This relationship, known as the Yerkes-Dodson curve, predicts that optimal performance occurs at intermediate levels of arousal (Aston-Jones and Cohen, 2005; Cools and D'Esposito, 2011; Murphy et al., 2011; Rajagovindan and Ding, 2011; Vijayraghavan et al., 2007; Yerkes and Dodson, 1908). But what are the synaptic and circuit mechanisms of this inverted-U dependence of optimal states for behavior and neural responses?

Reports on the cortical membrane potential dynamics associated with wakeful states have come to widely differing conclusion between species and sensory systems. Wakefulness is traditionally associated with low amplitude and arrhythmic scalp EEG. This canonical wakeful state has been referred to as the "activated" or "asynchronous" state, because excitatory neurons are thought to be tonically depolarized while interacting in a manner that reduces broad-ranging synchrony (Renart et al., 2010; Steriade et al., 2001; van Vreeswijk and Sompolinsky, 1996). Membrane potential recordings in awake cats support this view (Steriade et al., 2001), but recent work in rodent sensory cortical areas has revealed additional complexity. Membrane potentials in auditory cortex of rats have been found to be hyperpolarized and inactive across un-anesthetized states, though the arousal level of the animals was not quantified (Hromádka et al., 2008, 2013). Movement (walking or whisking) in mice is associated with cortical membrane potential dynamics akin to the "asynchronous" state in somatosensory, visual, and auditory cortical areas (Bennett et al., 2013; Crochet and Petersen, 2006; McGinley et al., 2013; Polack et al., 2013; Poulet and Petersen, 2008; Schneider et al., 2014; Zhou et al., 2014). However, while walking is associated with increases in stimulus-driven firing in the visual cortex (Bennett et al., 2013; Niell and Stryker, 2010; Polack et al., 2013), it is associated with decreases in sensory-evoked responses in the auditory cortex (McGinley et al., 2013; Schneider et al., 2014; Williamson et al., 2015; Zhou et al., 2014). During stillness, slow (2–10 Hz) fluctuations are prominent in the somatosensory cortex (Crochet and Petersen, 2006; Poulet and Petersen, 2008; Zagha et al., 2013), are of intermittent prominence in the visual cortex (Bennett et al., 2013; Polack et al., 2013; Reimer et al., 2014), and variably reported in the auditory cortex (Hromádka et al., 2008, 2013; Schneider et al., 2014; Zhou et al., 2014). One possible explanation of these apparently divergent results is that state (arousal) fluctuates continuously and rapidly, resulting in a high degree of variability between studies and between moments within individual studies, which has not been accounted for.

The diameter of the pupil and the occurrence of sharp-wave activity in the hippocampus are two well-established measures of arousal (Bradley et al., 2008; Buzsáki, 1986; Gilzenrat et al., 2010; Laeng et al., 2012; Reimer et al., 2014; Siegle et al., 2003; Vinck et al., 2015). Indeed, in rodents, measures of the pupil diameter have been used for binary classification of

"aroused" or "unaroused" states and predict differences in sensory response magnitude and reliability and the extent of slow fluctuations in visual cortical membrane potential (Reimer et al., 2014). We wondered if pupil diameter and hippocampal sharp-wave activity could be used to derive a continuous measure of arousal level, allowing study of the membrane potential dynamics associated with the inverted-U shaped dependence of signal detection task performance on arousal.

Here we report that the mouse's internal state fluctuates continuously and rapidly (in seconds or less), and arousal can be quantified simply as the diameter of the pupil. We find that pupil diameter closely tracks the rate of occurrence of hippocampal sharp waves. In addition, auditory cortical membrane potentials of layer 4 and 5 excitatory neurons exhibit: slowly fluctuating (1–10 Hz) rhythmic activity with low arousal, hyperpolarization and low variability at intermediate arousal, depolarization and variability with sustained hyper-arousal (with or without walking), and transient depolarization in synchrony with micro-arousal events. These results provide a framework with which to resolve apparent discrepancies between species and sensory systems in cortical membrane potential dynamics and reveal the membrane potential signature of optimal performance in a signal detection task. Substantial portions of this work have been presented previously in abstract form (McGinley et al., 2013, 2014).

RESULTS

We hypothesized that the arousal state of waking mice exhibits rapid moment-to-moment variations that impact behavior and cortical activity. We further hypothesized that there is an "optimal" state in which the behavioral performance of the animal on a task would peak and sensory responses would be large and reliable. Finally, we sought to determine the dynamic signature of membrane potential activity in the optimal sensory signal detection state. To this end, we trained mice in a challenging auditory tone-in-noise detection task and quantified the state of the mice in several conditions: (1) in the absence of sound exposure, (2) during passive listening to task stimuli (temporally orthogonal ripple combinations [TORCs]) (Atiani et al., 2009)), or (3) during the performance of an auditory task detecting tones embedded in these TORCs (see Experimental Procedures). To quantify state, we used pupillometry, rate of occurrence of sharp wave/ripple combinations and theta activity (θ/δ ratio; see Csicsvari et al., 1999) in the CA1 field of the hippocampus and spontaneous locomotor patterns on a cylindrical treadmill (Figures 1, S1, and S2). These measures relate to the internal state of the animal (Buzsáki, 1986; Loewenfeld, 1999; Reimer et al., 2014).

Brain State Varies Rapidly and Coherently with Pupil Diameter
Pupil diameter in waking mice varied widely on multiple time scales over the 1–3 hr recording/behavioral sessions (N = 41; n = 83), ranging from nearly pinpoint (∼0.15 mm) to nearly fully dilated (∼1.8 mm) in constant low-light conditions (see e.g., Figures 1B, 1C, 2A, 2B, 3A, 6A, 6C, S2, S4, and S5). Pupil dilations exhibited a broad range of periodicities and amplitudes, but three features were prominent: (1) frequent and brief (∼2 to 3 s duration) dilations (Figures 1C and 2), (2) slower constrictions

over periods of 5–30 s (Figures 1C and 3), and (3) nearly fully dilated pupils encompassing periods of walking (Figures 1B and 2A). We term the rapid, relatively brief dilations, "microdilations" to differentiate them from more prolonged changes in diameter. We detected microdilations by their rapid rate of rise of pupil diameter at their onset (see Experimental Procedures; Figures 1C and S4D).

To determine the relationship between the pupil diameter and brain state, we compared the moment-to-moment pupil diameter to fast ripples associated with sharp waves and theta activity in the hippocampus during spontaneous state changes in the absence of sensory stimulation (see Experimental Procedures). The pupil diameter exhibited a strong inverse relationship to the rate of occurrence of fast ripples (Figures 1C–1F and S1), with a peak coherence of 0.78 ± 0.07 (n = 6 cells from N = 6 animals) at low frequencies (<0.05 Hz) and a significant coherence at all frequencies up to 1 Hz (Figures 1E). Theta activity was largely associated with walking (Figures 1C, S1B, and S1C). These results support the view that pupil diameter may be a useful indicator of brain state (Murphy et al., 2011; Reimer et al., 2014; Vinck et al., 2015). To ensure that pupil dilations were not in response to changes in illumination due to eye movements, we also measured eyelid opening in darkness (Figure S2), since eyelid opening and pupil diameter are coupled together through co-innervation by the sympathetic nervous system (Loewenfeld, 1999). As expected, pupil dilation and eyelid opening fluctuated coherently, such that even in darkness (where pupil dilation is saturated) eyelid opening exhibited the same slow changes associated with walking or disengagement and micro-openings that are characteristic of pupil diameter (Figure S2; N = 7 animals). We also found that an easily measured proxy for changes in lid opening and pupil diameter is the amount of light reflected from the eye from an infrared light source, a measure we term eye-indexed state (EIS) (Figures 2A, 2B, and S2; N = 7). These results indicate that pupil dilation in constant illumination, eyelid opening in the dark, or EIS in either condition are precise, accurate, and easily obtained measures of brain state.

Large pupillary dilations, whisking, walking, and other movements frequently, but not always, occurred simultaneously as part of a larger realm of behavioral state changes, as observed previously (Mitchinson et al., 2011; Reimer et al., 2014; Schneider et al., 2014). We primarily focus on pupil diameter as a measure of state, owing to its ease of measurement, non-invasive nature, and ability to continuously and sensitively track state changes, whether or not they accompany overt walking, whisking, or other movements (see e.g., Movie S1). The maximal pupil diameter achieved during each recording or behavioral session always occurred during walking and varied, slightly, from day to day and animal to animal. Thus, to facilitate population-level comparisons and analysis, we normalized the pupil diameter by dividing by its maximal value in each session (see Figure 1B; see Experimental Procedures).

Cortical Membrane Potentials Track Changes in Brain State
Next we examined if pupil diameter/eyelid opening was related to the state of activity in auditory cortical neurons. We performed whole-cell recordings from auditory cortex (ACtx) layer 4 or 5
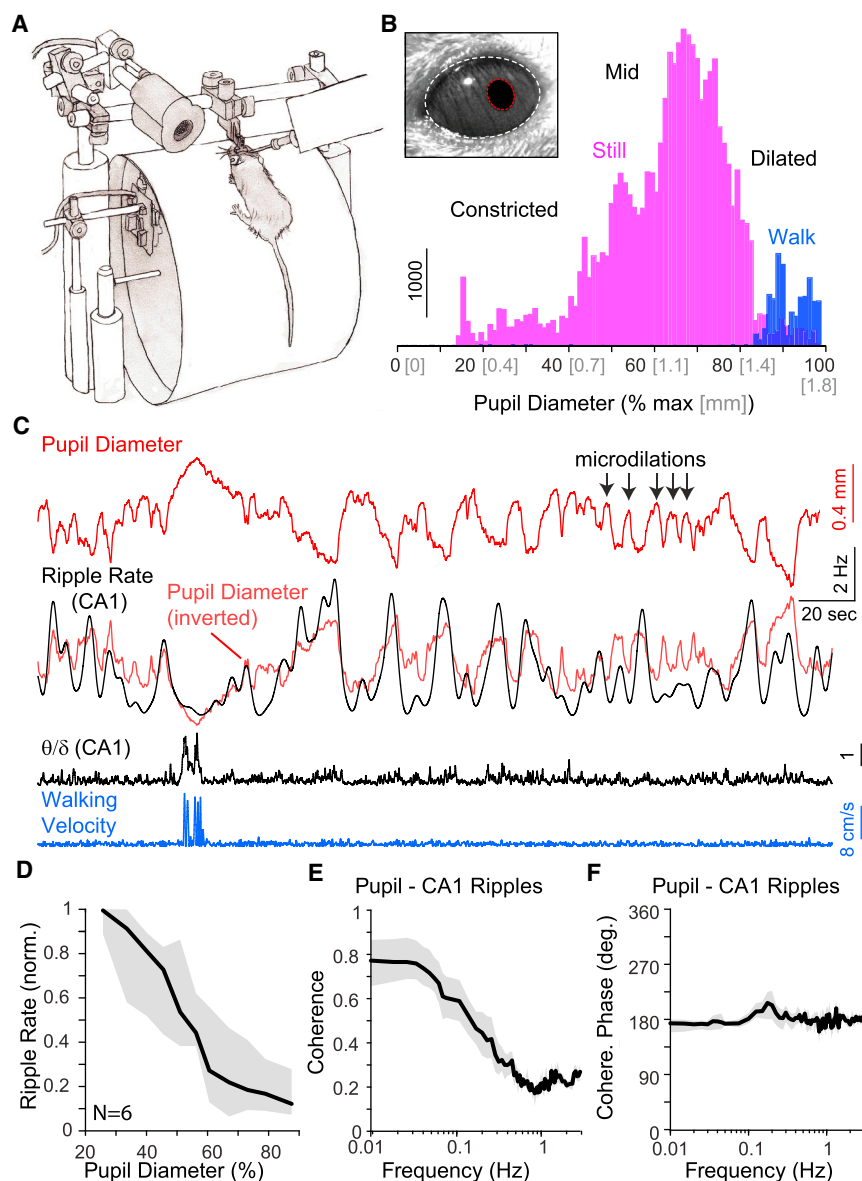
Figure 1. Peripheral and Central State Fluctuate Rapidly and Continuously in a Highly Correlated Manner in the Waking Mouse

(A) Head-fixed mice spontaneously stood or walked on a cylinder during whole-cell recordings from ACtx neurons.

(B) Pupil diameter was monitored via infrared camera and found to vary over a wide range (e.g., 0.3 to 1.8 mm in this animal) during the waking state.

(C) Pupil diameter is highly correlated with the rate of ripples in the CA1 area of the hippocampus. Light pink trace is an overlay of the inverted pupil diameter (upward = smaller pupil diameter) with rate of hippocampal ripples.

(D) Increased pupil diameter is associated with a large decrease in hippocampal ripple rate (R = −0.94 ± 0.03; N = 6). (E) Coherence between pupil dilation and CA1 ripple rate exhibits an average peak of 0.78 (N = 6) at low frequencies, demonstrating that pupil dilation is strongly associated with a decreased rate of occurrence of hippocampal ripples.

(F) The coherence between pupil diameter and ripple rate is consistently anti-phase (~180°) across the full range of relevant frequencies. Gray shaded areas indicate 68% confidence interval (CI).

pupillary dilator muscles (Loewenfeld, 1999). We performed detailed analysis of the nine recordings with long, stable membrane potential recordings, high-quality pupillometry data, and in which the pupil of the animal exhibited variation over a broad range of diameters. Membrane potential of cortical neurons exhibited a remarkably high coherence (calculated in a 200 s sliding window; see Experimental Procedures) with pupil diameter, peaking at 0.7 ± 0.1 at approximately 0.03 Hz (Figure 2C; n = 9). The close relationship between microdilations and transient depolarization was apparent as a peak in coherence at ~0.3 Hz, reflecting their seconds-long time course (Figure 2C).

In addition to a high correlation between cortical membrane potential and pupil diameter during microdilations, we also noted that in anticipation of a bout of walking, cortical membrane potential depolarized, followed (~1 s later) by large dilation of the pupil and finally (3 to 4 s later) walking (Figures 2 and S4). Walking was always associated with large diameter pupils (Figure 1B; see also Figure 6C), indicating that our animals only walked during high arousal states, and that the transition from still to walking is typically associated with a large change in arousal. Following the cessation of walking, the pupil diameter slowly constricted and cortical membrane potential slowly repolarized (n = 9; Figures 2 and S4). The changes in membrane potential we observed in cortical neurons with pupil dilations or walking did not result from disruptions of recording quality, since the membrane

presumed excitatory neurons (see Figure S3) in waking animals, measured spontaneous activity without sound presentation, and measured either pupil diameter (n = 9 neurons in N = 7 animals) or EIS (n = 7 neurons in N = 5 animals). Remarkably, the microdilations/micro-openings observed in still animals were reliably associated with 5–20 mV time-locked depolarization of cortical neuronal membrane potential (Figure 2; see also Figures 3 and S4; n = 16 neurons). These transient depolarizations preceded pupil dilation/eyelid opening by 1.1 ± 0.1 s (n = 16; see Figure 2C, inset). Much or all of this lag may represent the slow time course of pupillary/eyelid movement to alterations in sympathetic and parasympathetic activity (Loewenfeld, 1999). Microdilations were of a similar duration as the transient depolarizations (Figures 2A and 2B), and typically exhibited a rapid rise and a slower return to baseline (see e.g., Figures 2A, 2B, 3A, and S4D), suggestive of activation of the sympathetic innervation of
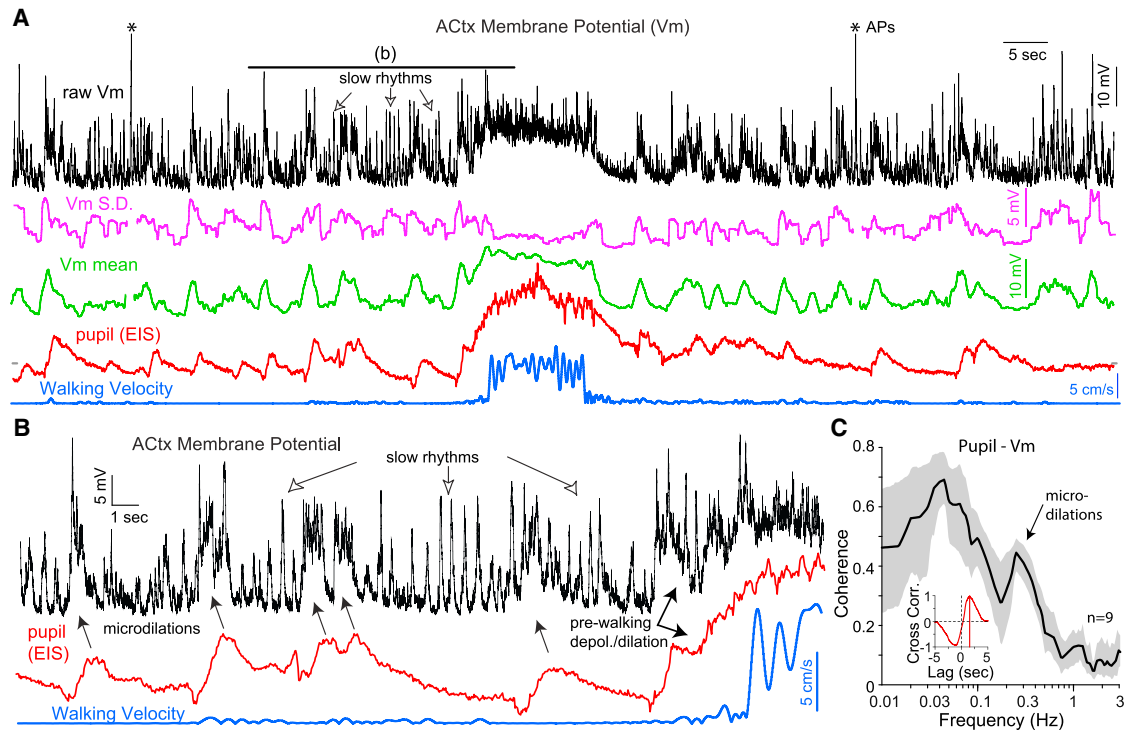
Figure 2. Global State Fluctuates Together with Cortical Membrane Potentials and Their Oscillations

An example ACtx membrane potential (Vm; top), the SD, and mean of the Vm in a 1 s sliding window (middle) and pupil dilation and walking patterns (bottom) on the same time base. Vm mean and SD are blanked during action potentials, indicated by asterisks at top. Brief periods of increased pupil diameter are highly correlated with depolarizations in the ACtx neuronal membrane potential. Just prior to and during walking, the membrane potential depolarizes and pupil diameter increase together. When pupil diameter becomes small, slow oscillatory synaptic activity becomes prominent. Note: the Vm SD and Vm mean are blanked during action potentials.

(B) Expansion in time of the relationship between neuronal membrane potential, pupil diameter, and walking. Note the brief depolarizations time-locked to pupil dilations.

(C) Coherence between pupil diameter and membrane potential exhibits an average peak of 0.68 (n = 9) at low frequencies (0.03 Hz) and a second peak at 0.3 Hz that corresponds to the brief periods of pupil dilation (microdilations). Depolarization of Vm preceded pupil dilation by 1.4 s, as indicated by the lag in the peak of the cross-correlation between pupil and Vm (inset), for the example trace shown in (A) and (B). Gray shaded area indicates 68% CI.

potential depolarization initiated prior to each behavioral event (e.g., dilation or walking) and always returned to pre-movement levels once movement or arousal ceased. Furthermore, spike threshold was only weakly correlated ($r = -0.16 \pm 0.08$) with pupil diameter and varied largely in relation to the rate-of-rise of the membrane potential leading up to action potential threshold, irrespective of pupillary or walking patterns (Figure S3H–S3J; see Experimental Procedures) (Azouz and Gray, 2000; McGinley and Oertel, 2006).

Cortical Membrane Potential and Variance Exhibit a U-shaped Dependence on Arousal

In addition to the high positive correlation between pupil diameter/eyelid microdilations and cortical neuronal membrane potential (e.g., Figures 2A and S4) that occurred during periods of intermediate to high arousal, additional features were apparent. Constricted pupil diameters (e.g., low arousal) were associated with slow rhythmic synaptic activity, resulting in high power in the low (2–10 Hz) and delta (1–4 Hz) frequency ranges, resulting in high membrane potential variance (see e.g., Figures 2A, 2B, 3A, S5, and S6). Dilation of the pupils from small toward interme-

diate diameters resulted in a strong suppression of this low-frequency synaptic activity, which in turn resulted in an average hyperpolarization of the membrane potential and a decrease in membrane potential variance (Figures 2A, 3A–3D, S5, and S6; n = 9). In contrast, dilation of the pupils from intermediate to larger diameters, with or without walking, were associated with an increase in the relative levels of higher (50–100 Hz) frequency fluctuations, an overall depolarization of the average membrane potential, and an increase in membrane potential variance (over intermediate arousal levels; Figures 3A–3D). Thus, plotting the membrane potential of cortical neurons as a group (n = 9) against arousal level revealed a U-shaped relationship between average membrane potential/variance with normalized pupil diameter (Figures 3C, S6A, and S6C). The smallest pupil diameters were associated with large variations in membrane potential (Figures 3B, 3D, and S6C), owing to the presence of slow (1–4 Hz and 2–10 Hz) rhythmic activity. Moderately dilated pupil diameters were associated with a significant decrease in membrane potential variance and an average hyperpolarization of the membrane potential (Figures 3C, 3D, S6A, and S6B), owing to a suppression of this slow
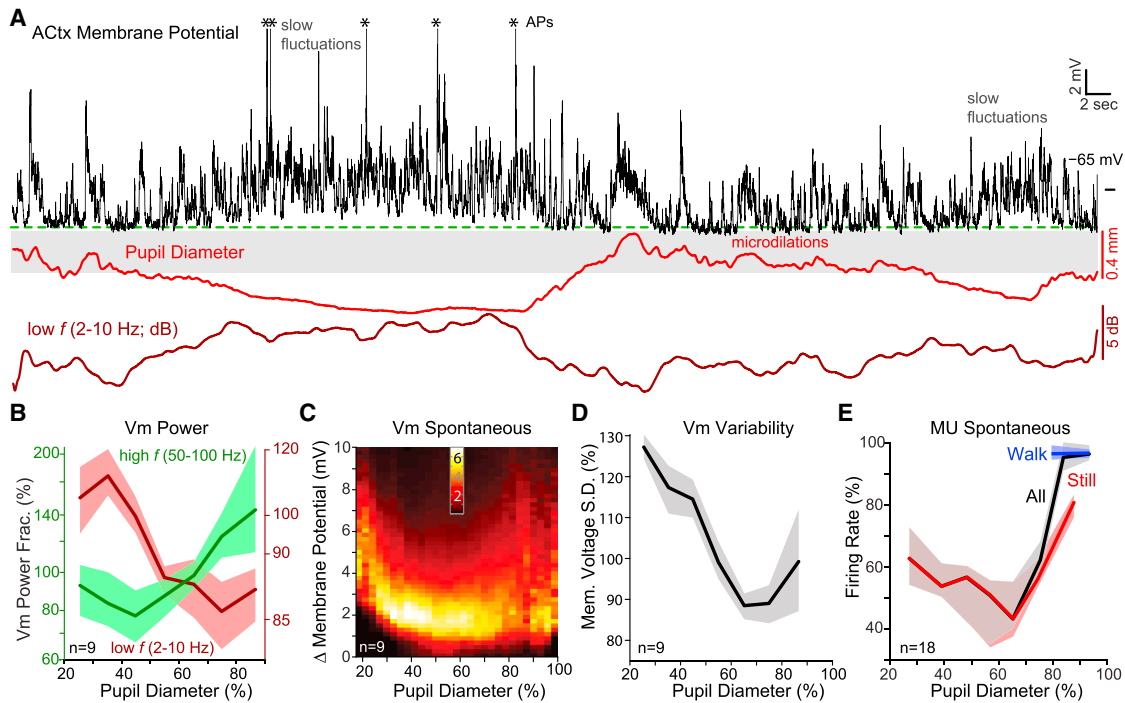
Figure 3. Neuronal Membrane Potentials and Their Variability Exhibit a U or an Inverted-U Relationship with Arousal, as Indexed by the Pupil Diameter

(A) As pupil diameter decreases below a critical zone (gray box), microdilations tend to stop and large fluctuations in synaptic activity at low (2–10 Hz) frequencies become prominent (at bottom). These low-frequency synaptic barrages are largely suppressed during pupil dilation, and the correlation between microdilations and brief depolarizations of the membrane potential are observed. At intermediate arousal when microdilations are absent, neurons are stably hyperpolarized (green horizontal dashed line). Asterisks indicate action potentials.

(B) Dependence of low-frequency and high-frequency Vm fluctuations on pupil diameter. Small diameters are associated with increased relative levels of low-frequency fluctuations in membrane potential, while large diameters are associated with increased relative levels of power at higher frequencies (see also Figure S6).

(C) 2D heatmap (each vertical slice normalized to an area of 100%) showing group data (n = 9 recordings) for the relationship between change in membrane potential from the minimum (lower bound of a 98% confidence interval) potential reached during the recording and normalized pupil diameter. Note that the membrane potential exhibits large variations for either small or large pupil dilations, with the smallest variability occurring at intermediate pupil dilation. Also note that membrane potentials are most hyperpolarized at intermediate pupil diameters. Zero "Δ Membrane Potential" corresponds to an average Vm of −74 ± 1.2 mV. Inset shows the color scale of the heatmap in % units.

(D) SD of membrane potential exhibits a non-monotonic relationship with pupil diameter.

(E) Spontaneous multiple unit (MU) firing rate in auditory cortex exhibits a U-shaped relationship with pupil diameter. Some of the increased unit activity with large pupils is associated with walking. Shaded areas indicate 68% CI.

rhythmic activity (Figure 3B and S6). States associated with larger pupil diameters (with or without walking) once again were associated with depolarization of the membrane potential and a higher degree of Vm variability (Figures 3A, 3C, 3D, and S6A–S6C; n = 9), owing to arrhythmic (at high frequencies) barrages of synaptic potentials.

The U-shaped relationship between Vm and pupil diameter resulted in a positive correlation between pupil diameter and Vm for intermediate to highly aroused states and a negative correlation between these measures at unaroused to intermediate arousal levels. This correlation pattern necessitated use of a sliding window when calculating Vm-to-pupil coherence (see Experimental Procedures). The state dependencies at the synaptic level were mirrored in layer 5 multi-unit (MU) activity, which exhibited a U-shaped relationship between pupil diameter and spontaneous neuronal discharge, with spontaneous activity being lowest at intermediate pupil diameters (Figure 3E;

n = 18). Hyper-arousal (large pupil diameter) was associated with an increase in spontaneous activity, and walking further increased this activity (Figure 3E).

Together, these results indicate that pupil diameter (which, in the absence of changes in luminance, is an indicator of sympathetic and parasympathetic activity) (Loewenfeld, 1999) is an accurate predictor of a wide range of brain state changes, well beyond those associated with walking or other movements, including the accumulation of torpor, micro arousals, sustained arousal, and hyper-arousal. This is true both in terms of sharp wave/ripple rate in the hippocampus, as well as membrane potential and variability (including rhythmic activity) of neocortical neurons. Owing to the association of walking with large pupil diameter (i.e., high arousal), previous studies on the effects of walking or other movements on sensory responses have most likely involved significant changes in arousal (Crochet and Petersen, 2006; Erisken et al., 2014; Fu et al., 2014; Niell and

Stryker, 2010; Otazu et al., 2009; Polack et al., 2013; Poulet and Petersen, 2008; Schneider et al., 2014; Schölvinck et al., 2015; Williamson et al., 2015; Zhou et al., 2014).

A recently published study of the mouse visual cortex, which paralleled our own investigations, suggested that the rate of change of pupil diameter was an accurate measure of changes in cortical membrane potential power (Reimer et al., 2014). To test whether pupil diameter or the rate of change of pupil diameter was a better indicator of rhythmic membrane potential activities, we compared both (1) raw pupil diameter and (2) the rate of change of pupil diameter to membrane power at 2–10 Hz and other frequency bands (Figures S5 and S6; Table S1). We found that pupil diameter explained 34% ± 7% (n = 9) of the variance in dB power at low frequencies (2–10 Hz), while the rate of change (temporal derivative) of pupil diameter explained approximately half as much variance (18% ± 4%; p < 0.005; $F_{1,7}$ = 28.3, group p < 0.001). Factoring in both the pupil diameter and its derivative explained 40% ± 6% of the variance of power in the 2–10 Hz band, which was statistically larger than the amount explained by pupil derivative (p < 0.0005) but not pupil diameter alone (p = 0.36). A similar pattern was observed for other frequency bands (Figure S6; Table S1). Importantly, we found that the derivative of the pupil was correlated to the pupil diameter 1.3 ± 0.7 s later (CC = 0.32 ± 0.02; p < 0.001; n = 9; Figures S6K and S6L) but not to the pupil diameter at the same time (correlation coefficient CC = 0.0035 ± 0.0043; p = 0.44). This lag approximately matched the observed lag between physiological activity and pupil diameter (see e.g., Figures 2B and 2C; Experimental Procedures), which reflects neural and muscle activation delays in the control of the pupil (Loewenfeld, 1999). These results suggest that some, and perhaps all, of the explanatory power of the pupil derivative occurs because it serves as a proxy for the pupil diameter approximately 1 s later. This is particularly the case during micro-dilations, when the pupil diameter fluctuates on approximately the same time scale (e.g., seconds) as the pupillary lag (see e.g., Figures 2A and 2C).

Auditory Cortical and Thalamic Sound Responses are Optimal at Intermediate Arousal

Given that sensory neural activity is known to be highly state dependent (Atiani et al., 2009; Fontanini and Katz, 2008; Issa and Wang, 2011; Livingstone and Hubel, 1981; Marguet and Harris, 2011; Niell and Stryker, 2010; Otazu et al., 2009; Zhou et al., 2014), we predicted that auditory evoked responses would be strongly correlated with our measure of state (pupil diameter) and would exhibit an optimal state. To test this hypothesis, we presented a sequence of six complex sounds (TORCs) in random order to mice trained in the detection task, while performing extracellular MU recordings (n = 18; N = 6) or whole-cell recordings from ACtx neurons targeted to layers 4 and 5 (Figure 4; n = 10, N = 5; 6 neurons with spiking, 6 with subthreshold activity isolated by hyperpolarizing the neuron by 10 mV with steady current, 2 neurons had both). Maximal whole-cell action potential responses were evoked on trials with moderate pupil diameters (Figure 4A, 4B, and S8; n = 6). Similarly, when recorded neurons were hyperpolarized by approximately 10 mV with the intracellular injection of current to prevent action potential generation, pupil diameter significantly influenced the ampli-

tude of stimulus evoked synaptic barrages. The largest synaptic responses were evoked at intermediate pupil diameters, with dilation or constriction from this resulting in smaller amplitude evoked synaptic responses (Figure 4C; n = 6). Comparing the average trial-to-trial cross-correlation (reliability) of the synaptic auditory cortical response across pupil diameters also revealed this to be highest at mid-pupil diameters (Figure 4D). MU recordings from putative layer 4 and 5 regular spiking neurons (n = 18 recording sites) confirmed and extended these findings (Figures 4E–4H). The cortical auditory MU response was state dependent, exhibiting an inverse-U relationship between pupil diameter and number of evoked action potentials (above baseline), reliability of evoked responses (trial-to-trial cross correlation), and response gain (Figure 4E–4G and S8). The maximal number of action potentials (over baseline) and the most reliable MU responses evoked by each stimulus occurred with mid-diameter pupils (Figures 4F, 4G, and S8). Comparing walking versus non-walking (still) with large pupil diameters revealed similar effects on evoked MU response, with no significant effects of walking per se over pupil-indexed arousal.

Does knowing the state of the animal help to explain trial-to-trial variability of the evoked action potential response? We sought to answer this question by comparing the increase in explained variance (relative to the variance explained by the identity of the TORC stimulus) by knowing (1) walking status, (2) pupil diameter, or (3) pupil diameter and walking status. While including the walking status increased the explained variance by 20% ± 8%, measuring the pupil diameter increased explained variance by 28% ± 8%, and including both walking status and pupil diameter increased explained variance by 29% ± 11% (Figure 4H; n = 12), which was significantly more than explained by walking alone, but not more than pupil alone. Thus, pupil diameter provided a good predictor of response variability in cortex that encompassed the predictive ability of walking status.

To examine if the variations in ACtx response amplitude also occurred at subcortical levels, we performed MU (n = 9) recordings in the medial geniculate (MG) body. As observed with ACtx neurons, variations in pupil diameter in the non-walking animal were associated with variations in the amplitude and reliability of the evoked action potential responses in MG neurons (Figures 5A–5C) but which were smaller in magnitude and had a distinct form. Increases in pupil diameter were associated with a steady decrease in MG response amplitude, and this response was further suppressed by a substantial amount during walking (Figure 5B, p < 0.005).

Previous studies have suggested that state changes may affect neuronal gain (Cohen and Maunsell, 2010; Goris et al., 2014; Otazu et al., 2009). To examine this hypothesis in our recordings, we determined the effect of pupil diameter on the gain and offset of ACtx (n = 18) and MG (n = 9) sound-evoked MU responses by comparing the relationship between responses sorted by pupil diameter versus responses averaged across all pupil diameters (Figures 5D–5H). If the state changes reflected by pupil diameter had no effect, this relationship would be a diagonal line with slope of 1. Variations in pupil diameter exhibited a consistent change in the slope of this relationship, with the highest slope occurring at intermediate pupil diameters (Figures 5D–5H) for both ACtx and MG responses (see, however,
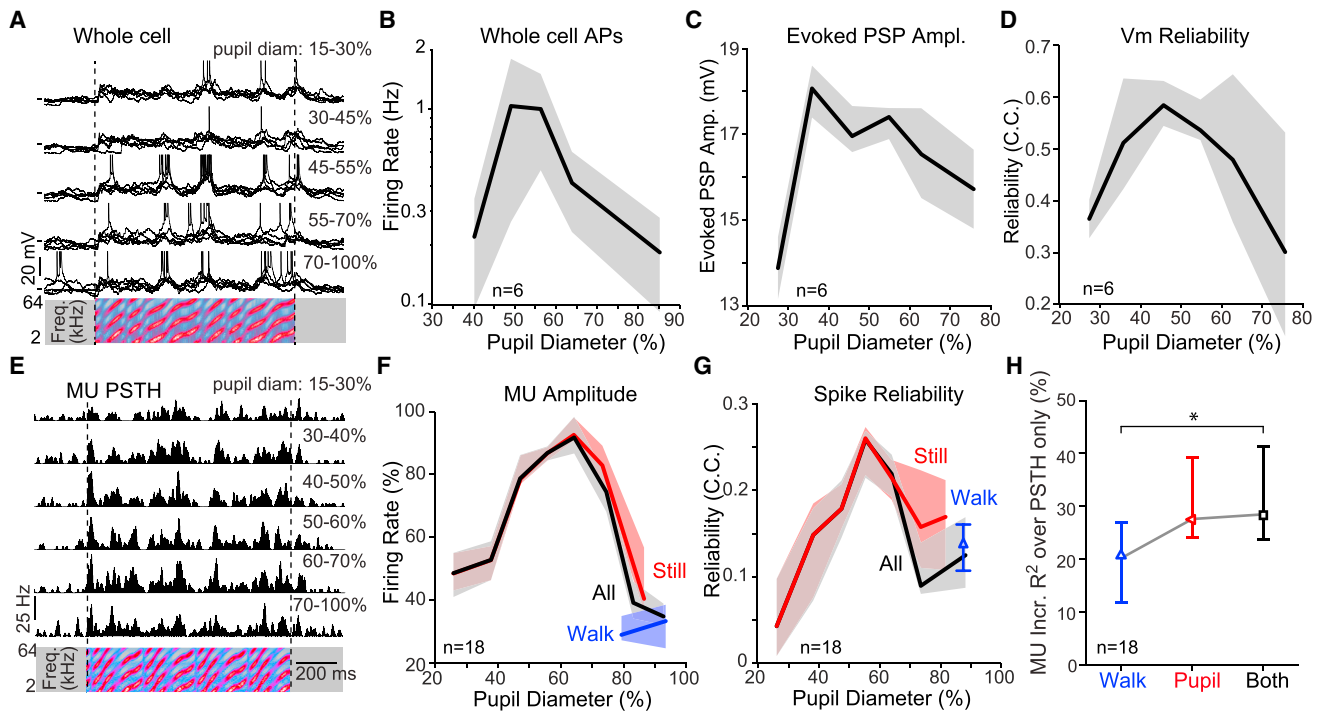
Figure 4. Subthreshold and Suprathreshold Evoked Responses in Auditory Cortex Are of Maximal Amplitude and Reliability at Intermediate Levels of Arousal

(A) Example whole-cell recording of responses to repeated presentation of a complex sound (TORC) sorted by pupil diameter. Sound presentation evokes the most spikes and largest, most reliable membrane potential depolarizations at intermediate pupil diameters. Tick marks on left are at the same membrane potential for reference.

(B) Group data (n = 6 recordings, N = 5 animals) illustrating that the maximal evoked action potential response in the Vm occurs at intermediate pupil dilation.

(C) Average TORC-evoked PSP amplitude (over baseline; see Experimental Procedures) peaks at intermediate pupil diameters.

(D) Reliability of synaptic responses (trial-to-trial cross-correlation of membrane potential) is highest at intermediate pupil dilations.

(E) Example PSTH responses of ACtx multiunit activity to a complex (TORC) sound are largest and most reliable at intermediate levels of pupil dilation.

(F) Group (n = 18 recordings, N = 6 animals) data illustrate that the average evoked firing rate is largest for intermediate pupil diameters. Both small and large pupil diameters are associated with decreased evoked (over spontaneous) responses. Walking is associated with decreased auditory responses, but to an extent not significantly different from responses during periods of non-walking with the same pupil diameters.

(G) Response reliability (average trial-to-trial cross correlation) is highest at mid-pupil diameters. Walking increases reliability over periods of non-walking with correspondingly large pupil diameters (p < 0.05).

(H) The increase in variance explained (over the PSTH alone) by incorporating walking status (left), pupil diameter (middle), or both (right). Incorporating both walking and pupil explains more variance than walking along, but not more than pupil diameter alone (n = 18; p < 0.05). Shaded areas indicate 68% CI.

Zhou et al., 2014). Smaller or larger pupil diameters away from this optimum were associated with decreases in the slope (gain) of this relationship. Thus, our measure of response gain (see Experimental Procedures), exhibited an inverse-U relationship with arousal for both MG and ACtx responses, as indexed by pupil diameter (Figures 5F and 5G). Comparing walking versus still with large pupil diameters revealed similar effects on MG spontaneous activity (Figure 5A) and MG response reliability (Figure 5C), but a stronger suppression of sound-evoked MG responses (Figure 5B; p < 0.002). Including the walking status increased the explained variance by 49% ± 15%, measuring the pupil diameter increased explained variance by 35% ± 13%, and including both walking status and pupil diameter increased explained variance in evoked discharge amplitude by 50% ± 9% (n = 9). These results are consistent with the large walking-specific decrease in evoked firing rate in MG neurons (Figure 5B) (Williamson et al., 2015).

Performance on an Auditory Detection Task Is Optimal at Intermediate Arousal

To examine how moment-to-moment variations in state affect the ability of animals to perform a Go/No-Go psychometric tone-in-noise detection task, we studied the pupil dependence of behavioral performance in mice that had been trained to detect the presence of a pure tone of variable intensity embedded in a complex sound (TORC; n = 30 sessions; N = 5 animals) (Figures 6B and S7) the same task animals were trained in before completing the above physiological experiments. We monitored the trial-to-trial variations in the ability to perform this go/no-go signal detection task in fully trained animals. Over 2 to 3 hr of behavior, trials in which the animal licked when a tone was present (Hits), did not lick when a tone was present (Misses), or licked when a tone was not present (False Alarms) were interspersed and highly variable (Figure 6A). As we expected, some variability in performance was
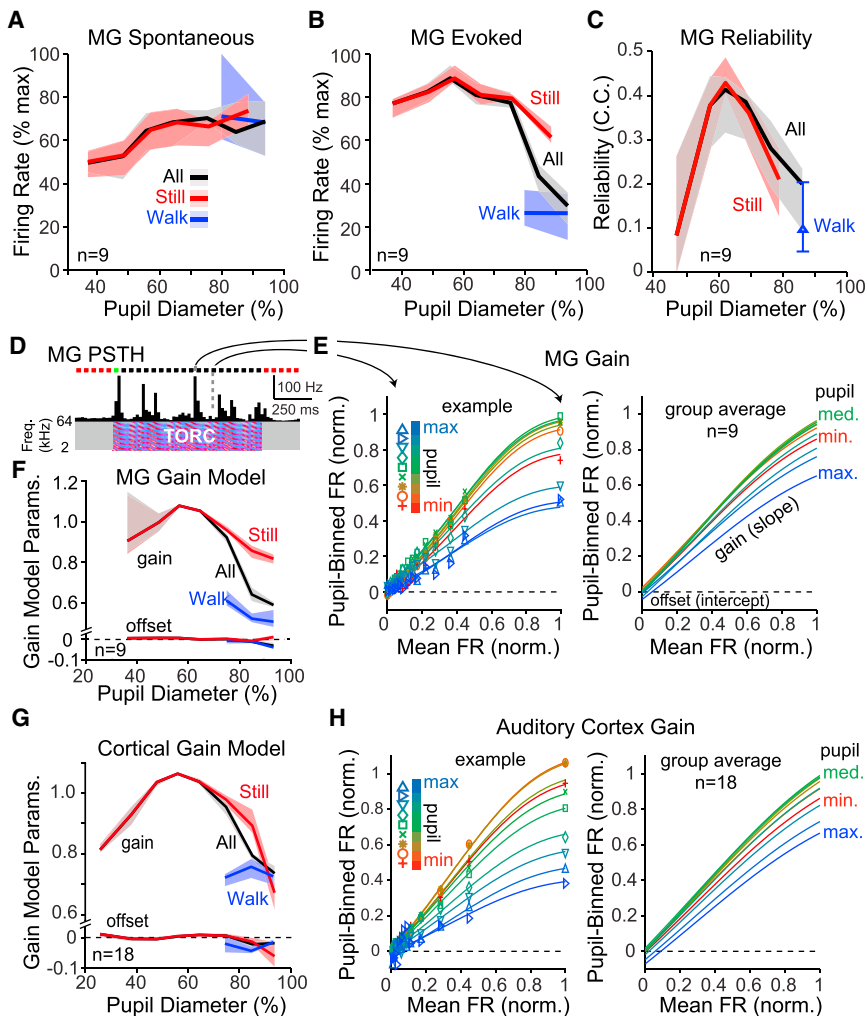
Figure 5. Cortical and Thalamic Gain Peaks at Intermediate Levels of Arousal

(A) Increases in pupil diameter are associated with modest increases in MU spontaneous activity in the MG. Walking was not associated with an additional increase in spontaneous activity compared to pupil dilation alone.

(B) TORC-evoked average firing rate over baseline peaks at intermediate pupil diameters and decreases with arousal. Walking is associated with a strong additional suppression of evoked MG responses.

(C) Reliability (trial-to-trial cross correlation) of MG responses peaks at intermediate pupil diameters.

(D) Example histogram of a MU MG response to a TORC stimulus.

(E and H) Average action potential counts in 20 ms bins were sorted and normalized from 0 (no spikes) to 1 (largest response) for the x axis. The data was then resorted according to pupil diameter (see Experimental Procedures) for the y axis. If arousal (pupil diameter) had no effect on response, then all the data should fit along the diagonal with a slope of 1. Both MG and ACtx responses were strongly affected by pupil diameter, with peak responses occurring at intermediate pupil diameters.

(F and G) Gain, as measured by our gain model (see Experimental Procedures), is modulated as changes in slope in MG (top) and cortex (bottom), while offset was relatively unchanged. This model is derived from un-binned data points and therefore differs slightly from the plots of (E) and (H), which are based on binned and averaged data for illustrative purposes (see Experimental Procedures). Shaded areas indicate 68% CI.

explained by the difficulty of individual trials associated with target intensity (Figures 6F and S7).

Over the course of a behavior session, pupil diameter also varied substantially (Figure 6A, bottom trace). We wondered if there was a relationship between pupil diameter and behavioral response. Indeed, plotting lick latency on hit trials against pupil diameter (average measured during the 500 ms prior to TORC onset) revealed a striking U-shaped relationship (Figures 6D, 6E, and S7). When the pupil was in the middle range, animals responded with the shortest and least variable latency. At smaller and larger pupil diameters, correct responses were more variable in timing and occurred at a longer latency on average (Figures 6D and 6E).

The ability of the animal to accurately perform the task was also highly state dependent. Hit rates exhibited an inverted-U relationship with pupil diameter, with the optimal hit rate occurring at intermediate pupil diameters for all tone intensities (Figures 6F, 6H, and S7). Interestingly, false alarm rate increased steadily with pupil diameter before plateauing at intermediate pupil diameters (Figures 6F and 6H). Sensitivity (d'), a measure of the ability to discriminate the presence of the tone, exhibited

an inverted-U relationship with pupil diameter, being maximal at small-to-intermediate pupil diameters, while bias (c; see Experimental Procedures) revealed a more symmetric U-shaped relationship, being minimal (closest to zero) at mid-pupil diameters (Figures 6G, 6I, and S7). These results reveal that trial-to-trial variations in behavioral response can be partially explained by trial-to-trial variations in behavioral state. Indeed, we found that knowing the pupil diameter resulted in a 37% ± 17%, 160% ± 120%, and 94% ± 55%; (N = 5; p < 0.05) increase in explained variance in estimating d', bias, and lick latency, respectively, over knowing the target-tone intensity alone (Figure 6J).

A dependence of performance on walking versus non-walking was largely, but not completely, predicted by pupil diameter. Walking, which was always accompanied by large pupil diameters (Figures 1B and 6C), was associated with a substantial increase in false alarms, a decrease in hit rate, and an increase in miss trials (Figures 6F–6H and S7I–S7L) in comparison to average non-walking periods. However, except for decision bias (Figure S7L), these effects of walking were not statistically significantly different from periods of non-walking that were associated with large pupil diameters (Figures 6E–6I).
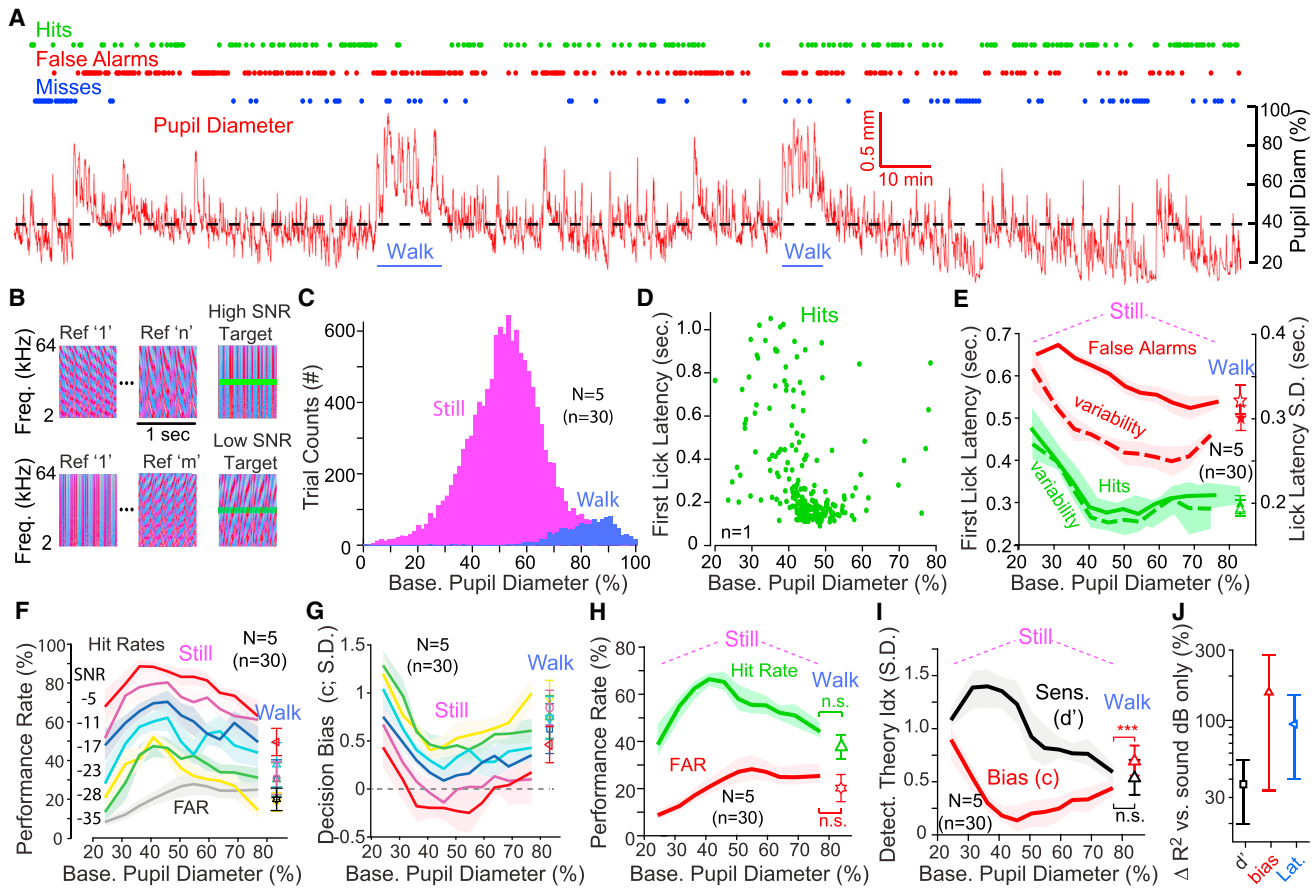
Figure 6. Sound Detection Performance Fluctuates Moment-to-Moment with State and Is Optimal at Intermediate Arousal Levels

(A) The ability of the animal to perform the auditory detection task and the pupil diameter vary widely throughout the training session. Note that false alarms appear prevalent because many more reference than target sound stimuli were presented (see Experimental Procedures).

(B) Example trial structure for the detection task. Mice were trained to lick for a reward upon detection of a pure tone embedded in a complex (TORC) sound. The level of the tone varied randomly from trial to trial. The frequency of the tone varied from day to day.

(C) Plotting pupil diameter over the course of the session revealed a broad range that centered around 50% diameter (N = 5 animals; n = 30 sessions). Walking was always associated with large pupil diameters.

(D) Plotting response latency on hit trials versus pupil diameter, for an example session, reveals that intermediate pupil diameters are associated with short latency licks and a large decrease in variability of lick latency.

(E) Group data demonstrating that lick latency on hit trials is shortest for intermediate pupil diameters (n = 30 sessions; N = 5 animals). On false alarm trials, lick latency from the start of the most recent TORC are significantly longer. Variability of lick latency (measured as average SD) is lowest at mid pupil diameters for both hit and false alarm responses (dashed lines and open symbols).

(F) Performance rate is maximal for intermediate pupil diameter for all tone levels, with the greatest modulation occurring between small and medium pupil diameters for quiet sounds. Increases in pupil diameter are associated with a large increase in false alarm rate (FAR).

(G) Decision bias (c) is minimal at intermediate pupil diameters for all tone levels.

(H and I) Group data, averaged across all tone levels, demonstrating that intermediate pupil diameters are associated with maximal hit rate and sensitivity and minimal bias. False alarm rate is reproduced from (F). Walking does not have additional effects to non-walking with large pupils, except for an additional increase in bias.

(J) Accounting for pupil diameter substantially increases the accuracy of estimates of d', bias, and latency over knowing tone intensity alone. Shaded areas indicate ± 1 SEM.

Comparing the pupil diameter at which performance peaked (Figures 6F and 6H) and lick latency was shortest (Figures 6D and 6E) with the distribution of pupil diameters over the course of the session (Figure 6C) revealed that the most frequently occurring pupil diameters were centered at or just above those associated with optimal behavioral performance. Thus, the rapid fluctuations in state reflected by the pupil were centered on one that was near optimal for performance of the task in well trained animals.

Cortical Membrane Potentials Are Stably Hyperpolarized before Correct Target Detections

Our results thus far have demonstrated that optimal supra- and sub-threshold sound responses and behavioral performance occur at intermediated arousal levels (Figures 4–6). In these intermediate arousal states, in passively awake animals that had been trained in the detection task, auditory cortical membrane potentials were stably hyperpolarized (Figures 2 and 3). To determine if similar membrane potential dynamics are associated with
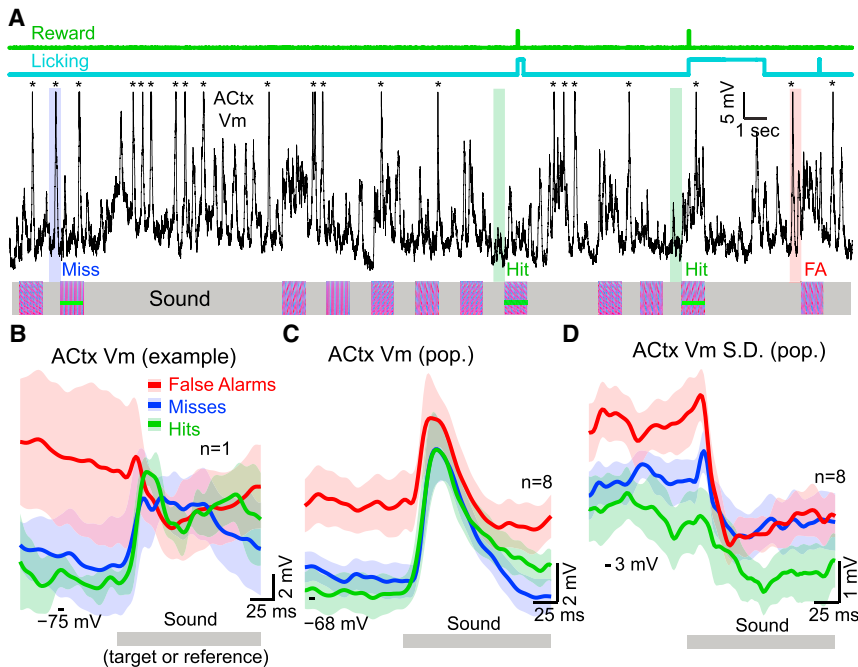
Figure 7. Auditory Cortical Membrane Potentials Are Most Hyperpolarized and Least Variable before Correct Target Identifications during the Detection Task

(A) An example membrane potential recorded during behavior. Lick patterns and reward administration are indicated at top. The sound spectrogram is recreated at bottom. Note horizontal green bars indicating the presence of target sounds and trial outcomes noted above. Asterisks indicate action potentials.

(B) The average membrane potential time course (± 1 SD) just before and after the start of sound, for all hits (green), misses (blue), and false alarms (FA; red) from an example recording during behavior.

(C) The average membrane potential trajectory sorted by trial type for the population of membrane potential recordings during behavior. Membrane potentials are hyperpolarized before hit trials, depolarized before false alarms, and intermediate before miss trials. Evoked responses are largest (from baseline) for hits and smallest for false alarms.

(D) The variability (SD) across trials of the membrane potentials, before and during the early component of sounds, is smallest for hit trials, largest for false alarms, and intermediate for miss trials. Data for Hit and Miss trials in (B)–(D) are resampled (1,000 times with replacement) to have equivalent target tone level distributions. Shaded areas indicate 68% CI unless noted.

arousal fluctuations during task engagement, we performed whole-cell recordings and measured eye-indexed state and hippocampal CA1 field potentials from animals performing the task (n = 8 cells; N = 5 animals). During behavior, the membrane potential of ACtx neurons exhibited periods of sustained hyperpolarization, brief depolarizations, slow fluctuations (2–10 Hz), and sustained depolarization that were associated with changes in eye indexed state (EIS) (see Figures 2, 3, and 7A). As predicted, membrane potentials were most hyperpolarized (p < 0.01 for hits versus FAs) and least variable (p < 0.01 for hits versus FAs) prior to hits (Figures 7B–7D). In addition, hit trials had the least variable membrane potentials during the early response to sound prior to onset of licking (Figure 7D; p < 0.05 for hits versus misses). Finally, the amplitude of evoked synaptic responses to the onset of the auditory stimulus (tone-in-TORC) were larger for hit versus false alarm trials (Figure 7C; p < 0.05). Thus, we conclude that a hyperpolarized and less variable cortical membrane potential is associated with an optimal state of readiness for sensory signal detection.

The precise peak pupil diameter of the U or inverted-U relationships differed slightly between particular behavioral and neural response measures (Figures 3–7). However, we did not find statistically significant difference between 12 of the 13 behavioral or physiological measures (hit rate, hit latency, c, ACtx reliability, ACtx amplitude, ACtx PSP amplitude, ACtx PSP reliability, Vm minimal value, Vm rest, ACtx spontaneous, MG amplitude, and MG reliability; Figure S8). Only our measure of peak behavioral discriminability, d', occurred at a significantly smaller pupil diameter than the other measures (Figure S8), possibly suggesting that optimal sound representations by auditory midbrain or brainstem structures occurs at slightly lower arousal

levels than optimal thalamo-cortical processing and behavioral execution. Overall, these results indicate that arousal levels associated with pupil diameters in the range of 40%–60% of fully dilated are optimal for both neural representation of auditory stimuli and behavioral performance in our auditory signal detection task.

DISCUSSION

Classical investigations of the effects of arousal on behavioral performance have revealed an inverted-U relationship: too little arousal results in "under performance," while hyper-arousal or excessive stress also impairs performance (Aston-Jones and Cohen, 2005; Cools and D'Esposito, 2011; Murphy et al., 2011; Rajagovindan and Ding, 2011; Vijayraghavan et al., 2007; Yerkes and Dodson, 1908). Our results suggest a cellular and network basis for this classical result. We found that intermediate arousal, as measured by pupillometry and hippocampal state, corresponded to a low noise cortical state, and optimal behavioral performance in a tone-in-noise detection task, and optimal thalamic and cortical sound responses. At intermediate arousal, behavioral performance was most rapid and accurate, sensory responses were largest and most reliable at both the spiking and subthreshold membrane potential levels, and spontaneous cortical membrane potentials were stably hyperpolarized. Thus, there was either an inverted-U- or U-shaped relationship between arousal and spontaneous or evoked auditory cortical activity (gain, amplitude, reliability, variance, etc.; Figures 2–5, 7, and 8) and behavior (response latencies, discrimination, bias, etc.; Figures 6–8). At the best state for behavioral performance on our sensory detection task, the signal-to-noise ratio
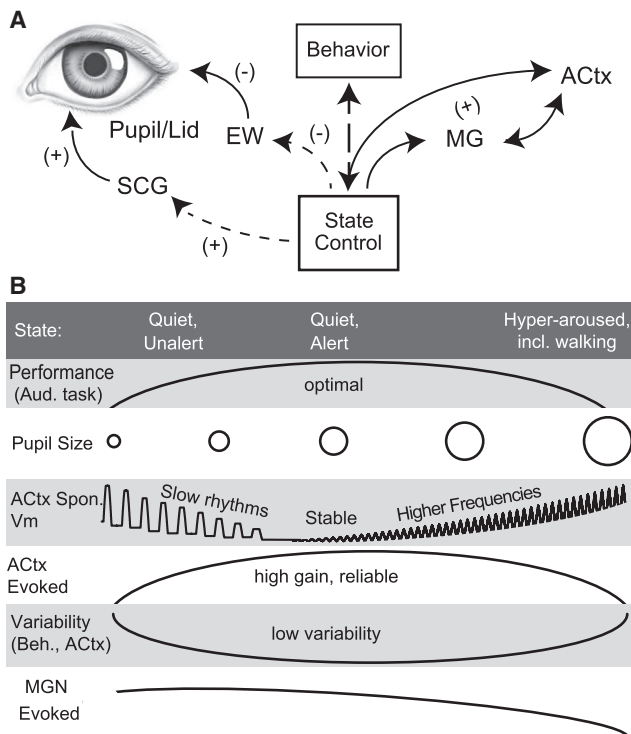
Figure 8. Influence of Internal State on Neuronal and Behavioral Accuracy and Responsiveness

(A) Brainstem/hypothalamic mechanisms of state control simultaneously modulate: pupil diameter, through the superior cervical ganglion (SCG) and the Edinger-Westphal (EW) nucleus; activity within the central auditory pathway, including the MG nucleus and primary auditory cortex (A1); and the animal's behavior.

(B) Relationship between state, behavioral performance, and auditory neural responsiveness. When pupil size is small, cortical slow-frequency oscillations are prominent (slow waves), resulting in low gain, low reliability of sound-evoked neuronal responses in the auditory cortex, and thus poor performance on the auditory detection task (low percent correct choices, frequent misses, variable latency behavioral responses). Moderate arousal (quiet, alert) is associated with a suppression of slow wave activity and an increase in the gain and reliability of auditory cortical evoked neuronal responses. Behavioral performance is optimal, with short latency, correct choices, and less variability. The hyper-aroused state (with or without walking), is associated with further ACtx neuronal depolarization, the appearance of fast as well as arrhythmic synaptic activity, and a decrease in MG-evoked responses. Together, these effects result in decreased amplitude and reliability of ACtx sound-evoked responses, and this is also reflected by diminished behavioral accuracy, with increased false alarms, misses, and more variable and longer response latencies.

of evoked cortical responses is high, owing both to the suppression of spontaneous activities and the enhanced amplitude of sensory-evoked responses (e.g., Figure 7C).

Increases in arousal from small pupil diameter (periods of drowsiness and/or inattentiveness) to moderate sized pupil (alert, attentive state) resulted in a suppression of ongoing slow oscillatory activity and subsequently an average hyperpolarization of Vm and a decrease in Vm variability (Figures 2, 3, and 8). We hypothesize that this suppression of low-frequency rhythms allows cortico-cortical and cortico-subcortical circuits

to operate more reliably, enhancing sensory-evoked neuronal interactions and thereby contributing to precise, reliable, and large sensory responses (Haider et al., 2010; Lee and Dan, 2012; Pinto et al., 2013).

High levels of arousal (reflected by large pupil diameters) were associated with a decrease in cortical sensory response amplitude/reliability and behavioral performance. The decreased sensory-evoked cortical response appears to result in part from decreased subcortical responsiveness, particularly during walking. Concomitant with this decreased subcortical gain, cortical neurons depolarized with hyper-arousal, entering what has been called the asynchronous or activated state (Renart et al., 2010; Steriade et al., 2001; van Vreeswijk and Sompolinsky, 1996). Although depolarization may increase the responsiveness of single cortical neurons, it may have a detrimental effect on sensory-evoked neuronal interactions if the depolarization is mediated by synaptic activity that increases membrane variance or is unrelated to the task. The subsequent decreased reliability of cortical responses may also decrease the amplitude of their sensory-evoked responses by disrupting the optimal spatiotemporal interactions of task-related cortical circuits. We propose that together these opposing arousal-associated changes in thalamo-cortical activity produce the U, or inverted U, shaped relationships between neuronal and behavioral responses and arousal observed here (Figure 8). Further examination of this hypothesis, particularly the influence of behavioral context (e.g., detection versus discrimination or exploration-exploitation tradeoffs), remains to be done.

Are the effects of arousal similar across cortical areas? In studies of the visual cortex, locomotion is associated with enhanced sensory-evoked visual responses (over non-locomotion) (Bennett et al., 2013; Niell and Stryker, 2010; Polack et al., 2013), while in auditory cortex locomotion results in significant suppression of sensory-evoked responses (McGinley et al., 2013; Schneider et al., 2014; Williamson et al., 2015; Zhou et al., 2014). It is currently unclear whether these apparently opposing results reflect variations between sensory systems in cortical or subcortical influences of locomotion and/or arousal, or differences in the state of the animal such as the arousal level during stillness. Indeed, our results indicate that the often reported effects of movement may not result from movement (e.g., whisking or walking) per se, but rather from arousal. In our animals, walking necessarily involved strong arousal (pupil dilation), and we observed largely similar effects on neural responses and behavioral performance of high arousal during either stillness or walking (Figures 2–6), with the exception of an arousal-independent walking effect on thalamic sound responses and decision bias.

Another possible source of variation between studies of locomotion or arousal effects is the laminar position and cell type of the recorded neurons. In the auditory cortex, depth of anesthesia affects pyramidal cell sensory-evoked responses and spontaneous activity differentially between cortical layers (Sakata and Harris, 2009), and the actions of neuromodulatory transmitters are layer and cell type specific (McCormick, 1992). Indeed, while our deep lying pyramidal neurons were depolarized during micro-arousals without walking (Figure 2), whole-cell recordings from layer 2/3 pyramidal cells in the visual cortex reveal no

significant change in membrane potential with non-movement related arousal (Reimer et al., 2014).

Two recent studies of mouse visual cortex have also revealed the powerful effects of arousal, as indexed by pupil diameter, on spontaneous activity and sensory-evoked effects in the absence of movement (Reimer et al., 2014; Vinck et al., 2015). Moments when the pupil diameter was increasing were associated with a decrease in low-frequency oscillations in visual cortical neuronal membrane potential and enhanced neuronal responses, both in amplitude and reliability, to sensory stimuli compared to moments when the pupil was decreasing in diameter (Reimer et al., 2014). These variations in arousal not only influence the prevalence of low-frequency rhythmic activities in local cortical circuits, but also have a strong influence on the correlational activity (e.g., noise correlations) between simultaneously recorded neurons (Vinck et al., 2015).

What pathways are responsible for moment-to-moment changes in arousal? Pharmacological investigations indicate that arousal-performance relationships operate at least in part through the activation of central adrenergic receptors (Vijayraghavan et al., 2007). Activation of adrenergic receptors can potently suppress cortical slow rhythms, depolarize layer 5 pyramidal cells, and increase neuronal excitability (McCormick, 1992). Indeed, whole-cell recordings from neurons in the visual cortex of wakeful mice reveal a small, sustained depolarization with walking that is associated with decreased membrane variance (Bennett et al., 2013), which is eliminated during blockade of cortical adrenergic receptors (Polack et al., 2013). A widely reported recording from a primate locus coeruelus (LC) neuron found a strong relationship between activity in this noradrenergic cell and pupil dilation (Aston-Jones and Cohen, 2005), suggesting that the LC may couple together brain state with pupil diameter. However, multiple neurotransmitter systems are involved in the control of activity in cortical and thalamocortical networks (Lee and Dan, 2012; McCormick et al., 2015) and are likely to be involved in the neural mechanisms underlying the effects observed here.

One possible circuit involved in arousal-associated changes in cortical responsiveness is the cholinergic activation of inhibitory interneurons in layer 1, whose activity inhibits the activity of other classes of interneurons in layers 2/3 (Fu et al., 2014; Lee et al., 2013; Pi et al., 2013). Another possibility is enhanced inhibition through cortico-cortical activation of parvalbumin neurons (Schneider et al., 2014). Through these, or similar, mechanisms, activation of cholinergic (or possibly serotoninergic) pathways can result in the disinhibition of cortical pyramidal cells and their dendrites, shifting the balance of excitation and inhibition to alter neuronal responsiveness to sensory stimuli (Wehr and Zador, 2003; Zhou et al., 2014). The influence of norepinephrine, which is thought to control pupil diameter (Aston-Jones and Cohen, 2005), on cortical inhibitory circuits remains to be determined.

Our results suggest that moment-to-moment fluctuations in arousal, reflected by pupil diameter, predict behavioral states that are conducive or detrimental to accurate sensation and action. We hypothesize that these rapid fluctuations in state may account for a significant fraction of the well-known trial-to-trial variability of sensory responses (Cohen and Maunsell, 2010; Goris et al., 2014; Kelly et al., 2010; Livingstone and Hubel, 1981; Tolhurst et al., 1983). Indeed, knowing the pupil-indexed state during presentation of an auditory stimulus in our animals explained comparable variation in the cortical neuronal response and behavioral performance to knowing which auditory stimulus had been presented. In support of this observation, recent investigations of visual, somatosensory, and auditory cortical responses in rodents have revealed physiological variability associated with rapid switching between disengaged (e.g., still) and active (e.g., movement) states (Bennett et al., 2013; Erisken et al., 2014; Fontanini and Katz, 2008; Polack et al., 2013; Poulet and Petersen, 2008; Reimer et al., 2014; Schneider et al., 2014; Schölvinck et al., 2015; Vinck et al., 2015; Vyazovskiy et al., 2011; Zagha et al., 2013; Zhou et al., 2014).

Are our findings relevant to human studies of arousal and task performance? The human pupil is reactive to emotional and cognitive state, and has been used to infer the person's level of arousal, attentiveness, cognitive load or brain-wide "gain" (Bradley et al., 2008; Eldar et al., 2013; Gilzenrat et al., 2010; Jepma and Nieuwenhuis, 2011; Murphy et al., 2011). Similar to our results, human pre-stimulus pupil diameter exhibits a U-shaped relationship with reaction time in performing an auditory "oddball" detection task (i.e., shortest reaction times at intermediate pupil diameters). Likewise, the largest P3 event-related potential was also evoked at these intermediate pre-stimulus pupil diameters (Murphy et al., 2011). Pupillary changes have also been used to indicate momentary periods of inattentiveness in humans (Kristjansson et al., 2009).

Revealing the neural mechanisms by which the state of the brain and periphery is controlled on a moment-to-moment basis promises to clarify many interesting aspects of neural network function, including the neural basis of optimal performance, and may reveal a nervous system that is considerably more accurate and less variable than previously thought.

EXPERIMENTAL PROCEDURES

All procedures were carried out in accordance with Yale University Institutional Animal Care and Use Committee. A head post was affixed to the skull of 7-week-old wild-type mice prior to ~1 month of acclimation to the experimental training setup and training in the signal detection task. A craniotomy was then made over ACtx or MG, and animals were allowed to recover for 2 to 3 days prior to recording (see Supplemental Experimental Procedures: Surgical Procedures). All animals were trained in a psychometric tone-in-noise detection task with sugar water reward for licking during targets and a timeout for incorrect licks (see Supplemental Experimental Procedures: Behavioral Training). Sounds were presented free field to the contralateral ear (see Supplemental Experimental Procedures: Sound Presentation). The arousal state of the mice was determined using infrared imaging of the pupil and eye lid and/or laminar field potential recording of fast ripples associated with sharp waves in the hippocampus (see Supplemental Experimental Procedures: State Monitoring).

Whole-cell recordings were made from regular or fast spiking neurons in layers 4 and 5 of ACtx using a physiological intracellular solution (see Supplemental Experimental Procedures: Whole-Cell Recording). Extracellular MU recordings were made in ACtx or MG using single tungsten electrodes (see Supplemental Experimental Procedures: Extracellular Recording). A state-dependent gain model was applied to MU recording data from ACtx and MG by binning the pupil diameter and determining the gain and offset for each pupil bin which, when applied to the PSTH, explained the most real variance in sound responses. The reliability of the physiological responses to sounds was calculated for each pupil bin as the average of the correlation coefficient between all pairs of responses to the same sound (see Supplemental Experimental Procedures: Gain Model and Reliability and Explained Variance).

Behavioral performance in the detection task was assessed using response times and standard signal detection theory measures applied for each pupil bin and target sound level (see Supplemental Experimental Procedures: Behavioral Performance Measures). Statistical inferences were made using parametric or non-parametric statistics and ANOVA models with posthoc pairwise comparisons, as appropriate, and data are presented as SD, SEM, or the width of a 68% bootstrap confidence interval, based on the normality of the data distributions and whether illustrations are intended to communicate confidence in the mean or the variability in the data, as appropriate (see Supplemental Experimental Procedures: Statistics and Analysis).

SUPPLEMENTAL INFORMATION

Supplemental Information includes eight figures, one table, one movie, and Supplemental Experimental Procedures and can be found with this article online at http://dx.doi.org/10.1016/j.neuron.2015.05.038.

AUTHOR CONTRIBUTIONS

ACKNOWLEDGMENTS

REFERENCES

Aston-Jones, G., and Cohen, J.D. (2005). An integrative theory of locus coeruleus-norepinephrine function: adaptive gain and optimal performance. Annu. Rev. Neurosci. 28, 403–450.

Atiani, S., Elhilali, M., David, S.V., Fritz, J.B., and Shamma, S.A. (2009). Task difficulty and performance induce diverse adaptive patterns in gain and shape of primary auditory cortical receptive fields. Neuron 61, 467–480.

Azouz, R., and Gray, C.M. (2000). Dynamic spike threshold reveals a mechanism for synaptic coincidence detection in cortical neurons in vivo. Proc. Natl. Acad. Sci. USA 97, 8110–8115.

Bennett, C., Arroyo, S., and Hestrin, S. (2013). Subthreshold mechanisms underlying state-dependent modulation of visual responses. Neuron 80, 350–357.

Bradley, M.M., Miccoli, L., Escrig, M.A., and Lang, P.J. (2008). The pupil as a measure of emotional arousal and autonomic activation. Psychophysiology 45, 602–607.

Buzsáki, G. (1986). Hippocampal sharp waves: their origin and significance. Brain Res. 398, 242–252.

Cohen, M.R., and Maunsell, J.H. (2010). A neuronal population measure of attention predicts behavioral performance on individual trials. J. Neurosci. 30, 15241–15253.

Cools, R., and D'Esposito, M. (2011). Inverted-U-shaped dopamine actions on human working memory and cognitive control. Biol. Psychiatry 69, e113–e125.

Crochet, S., and Petersen, C.C. (2006). Correlating whisker behavior with membrane potential in barrel cortex of awake mice. Nat. Neurosci. 9, 608–610.

Csicsvari, J., Hirase, H., Czurkó, A., Mamiya, A., and Buzsáki, G. (1999). Oscillatory coupling of hippocampal pyramidal cells and interneurons in the behaving Rat. J. Neurosci. 19, 274–287.

Eldar, E., Cohen, J.D., and Niv, Y. (2013). The effects of neural gain on attention and learning. Nat. Neurosci. 16, 1146–1153.

Erisken, S., Vaiceliunaite, A., Jurjut, O., Fiorini, M., Katzner, S., and Busse, L. (2014). Effects of locomotion extend throughout the mouse early visual system. Curr. Biol. 24, 2899–2907.

Fontanini, A., and Katz, D.B. (2008). Behavioral states, network states, and sensory response variability. J. Neurophysiol. 100, 1160–1168.

Fu, Y., Tucciarone, J.M., Espinosa, J.S., Sheng, N., Darcy, D.P., Nicoll, R.A., Huang, Z.J., and Stryker, M.P. (2014). A cortical circuit for gain control by behavioral state. Cell 156, 1139–1152.

Gilzenrat, M.S., Nieuwenhuis, S., Jepma, M., and Cohen, J.D. (2010). Pupil diameter tracks changes in control state predicted by the adaptive gain theory of locus coeruleus function. Cogn. Affect. Behav. Neurosci. 10, 252–269.

Goris, R.L., Movshon, J.A., and Simoncelli, E.P. (2014). Partitioning neuronal variability. Nat. Neurosci. 17, 858–865.

Haider, B., Krause, M.R., Duque, A., Yu, Y., Touryan, J., Mazer, J.A., and McCormick, D.A. (2010). Synaptic and network mechanisms of sparse and reliable visual cortical activity during nonclassical receptive field stimulation. Neuron 65, 107–121.

Hromádka, T., Deweese, M.R., and Zador, A.M. (2008). Sparse representation of sounds in the unanesthetized auditory cortex. PLoS Biol. 6, e16.

Hromádka, T., Zador, A.M., and DeWeese, M.R. (2013). Up states are rare in awake auditory cortex. J. Neurophysiol. 109, 1989–1995.

Issa, E.B., and Wang, X. (2011). Altered neural responses to sounds in primate primary auditory cortex during slow-wave sleep. J. Neurosci. 31, 2965–2973.

Jepma, M., and Nieuwenhuis, S. (2011). Pupil diameter predicts changes in the exploration-exploitation trade-off: evidence for the adaptive gain theory. J. Cogn. Neurosci. 23, 1587–1596.

Kelly, R.C., Smith, M.A., Kass, R.E., and Lee, T.S. (2010). Local field potentials indicate network state and account for neuronal response variability. J. Comput. Neurosci. 29, 567–579.

Kristjansson, S.D., Stern, J.A., Brown, T.B., and Rohrbaugh, J.W. (2009). Detecting phasic lapses in alertness using pupillometric measures. Appl. Ergon. 40, 978–986.

Laeng, B., Sirois, S., and Gredebäck, G. (2012). Pupillometry: A window to the preconscious? Perspect. Psychol. Sci. 7, 18–27.

Lee, S.H., and Dan, Y. (2012). Neuromodulation of brain states. Neuron 76, 209–222.

Lee, S., Kruglikov, I., Huang, Z.J., Fishell, G., and Rudy, B. (2013). A disinhibitory circuit mediates motor integration in the somatosensory cortex. Nat. Neurosci. 16, 1662–1670.

Livingstone, M.S., and Hubel, D.H. (1981). Effects of sleep and arousal on the processing of visual information in the cat. Nature 291, 554–561.

Loewenfeld, I.E. (1999). The Pupil. Anatomy, Physiology, and Clinical Applications, Volume 1 (Boston: Butterworth Heinemann).

Marguet, S.L., and Harris, K.D. (2011). State-dependent representation of amplitude-modulated noise stimuli in rat auditory cortex. J. Neurosci. 31, 6414–6420.

McCormick, D.A. (1992). Neurotransmitter actions in the thalamus and cerebral cortex. J. Clin. Neurophysiol. 9, 212–223.

McCormick, D.A., McGinley, M.J., and Salkoff, D.B. (2015). Brain state dependent activity in the cortex and thalamus. Curr. Opin. Neurobiol. 31, 133–140.

McGinley, M.J., and Oertel, D. (2006). Rate thresholds determine the precision of temporal integration in principal cells of the ventral cochlear nucleus. Hear. Res. 216-217, 52–63.

McGinley, M.J., David, S.V., and McCormick, D.A. (2013). Modulation of spontaneous and sensory-evoked synaptic dynamics in A1 during auditory discrimination tasks in mice. In Society for Neuroscience annual meeting.

McGinley, M.J., David, S.V., and McCormick, D.A. (2014). Predicting cortical response variability in awake-behaving mice: the role of arousal, behavioral performance, and auditory stimuli. Association for Research in Otolaryngology abstracts.

Mitchinson, B., Grant, R.A., Arkley, K., Rankov, V., Perkon, I., and Prescott, T.J. (2011). Active vibrissal sensing in rodents and marsupials. Philos. Trans. R. Soc. Lond. B Biol. Sci. 366, 3037–3048.

Murphy, P.R., Robertson, I.H., Balsters, J.H., and O'connell, R.G. (2011). Pupillometry and P3 index the locus coeruleus-noradrenergic arousal function in humans. Psychophysiology 48, 1532–1543.

Niell, C.M., and Stryker, M.P. (2010). Modulation of visual responses by behavioral state in mouse visual cortex. Neuron 65, 472–479.

Otazu, G.H., Tai, L.H., Yang, Y., and Zador, A.M. (2009). Engaging in an auditory task suppresses responses in auditory cortex. Nat. Neurosci. 12, 646–654.

Pi, H.J., Hangya, B., Kvitsiani, D., Sanders, J.I., Huang, Z.J., and Kepecs, A. (2013). Cortical interneurons that specialize in disinhibitory control. Nature 503, 521–524.

Pinto, L., Goard, M.J., Estandian, D., Xu, M., Kwan, A.C., Lee, S.H., Harrison, T.C., Feng, G., and Dan, Y. (2013). Fast modulation of visual perception by basal forebrain cholinergic neurons. Nat. Neurosci. 16, 1857–1863.

Polack, P.O., Friedman, J., and Golshani, P. (2013). Cellular mechanisms of brain state-dependent gain modulation in visual cortex. Nat. Neurosci. 16, 1331–1339.

Poulet, J.F., and Petersen, C.C. (2008). Internal brain state regulates membrane potential synchrony in barrel cortex of behaving mice. Nature 454, 881–885.

Rajagovindan, R., and Ding, M. (2011). From prestimulus alpha oscillation to visual-evoked response: an inverted-U function and its attentional modulation. J. Cogn. Neurosci. 23, 1379–1394.

Reimer, J., Froudarakis, E., Cadwell, C.R., Yatsenko, D., Denfield, G.H., and Tolias, A.S. (2014). Pupil fluctuations track fast switching of cortical states during quiet wakefulness. Neuron 84, 355–362.

Renart, A., de la Rocha, J., Bartho, P., Hollender, L., Parga, N., Reyes, A., and Harris, K.D. (2010). The asynchronous state in cortical circuits. Science 327, 587–590.

Sakata, S., and Harris, K.D. (2009). Laminar structure of spontaneous and sensory-evoked population activity in auditory cortex. Neuron 64, 404–418.

Schneider, D.M., Nelson, A., and Mooney, R. (2014). A synaptic and circuit basis for corollary discharge in the auditory cortex. Nature 513, 189–194.

Schölvinck, M.L., Saleem, A.B., Benucci, A., Harris, K.D., and Carandini, M. (2015). Cortical state determines global variability and correlations in visual cortex. J. Neurosci. 35, 170–178.

Siegle, G.J., Steinhauer, S.R., Stenger, V.A., Konecky, R., and Carter, C.S. (2003). Use of concurrent pupil dilation assessment to inform interpretation and analysis of fMRI data. Neuroimage 20, 114–124.

Steriade, M., Timofeev, I., and Grenier, F. (2001). Natural waking and sleep states: a view from inside neocortical neurons. J. Neurophysiol. 85, 1969–1985.

Tolhurst, D.J., Movshon, J.A., and Dean, A.F. (1983). The statistical reliability of signals in single neurons in cat and monkey visual cortex. Vision Res. 23, 775–785.

van Vreeswijk, C., and Sompolinsky, H. (1996). Chaos in neuronal networks with balanced excitatory and inhibitory activity. Science 274, 1724–1726.

Vijayraghavan, S., Wang, M., Birnbaum, S.G., Williams, G.V., and Arnsten, A.F. (2007). Inverted-U dopamine D1 receptor actions on prefrontal neurons engaged in working memory. Nat. Neurosci. 10, 376–384.

Vinck, M., Batista-Brito, R., Knoblich, U., and Cardin, J.A. (2015). Arousal and locomotion make distinct contributions to cortical activity patterns and visual encoding. Neuron 86, 740–754.

Vyazovskiy, V.V., Olcese, U., Hanlon, E.C., Nir, Y., Cirelli, C., and Tononi, G. (2011). Local sleep in awake rats. Nature 472, 443–447.

Wehr, M., and Zador, A.M. (2003). Balanced inhibition underlies tuning and sharpens spike timing in auditory cortex. Nature 426, 442–446.

Williamson, R.S., Hancock, K.E., Shinn-Cunningham, B.G., and Polley, D.B. (2015). Locomotion and task demands differentially modulate thalamic audiovisual processing during active search. Current Biology 26, in press.

Yerkes, R.M., and Dodson, J.D. (1908). The relation of strength of stimulus to rapidity of habit-formation. J. Comp. Neurol. Psychol. 18, 459–482.

Zagha, E., Casale, A.E., Sachdev, R.N., McGinley, M.J., and McCormick, D.A. (2013). Motor cortex feedback influences sensory processing by modulating network state. Neuron 79, 567–578.

Zhou, M., Liang, F., Xiong, X.R., Li, L., Li, H., Xiao, Z., Tao, H.W., and Zhang, L.I. (2014). Scaling down of balanced excitation and inhibition by active behavioral states in auditory cortex. Nat. Neurosci. 17, 841–850.